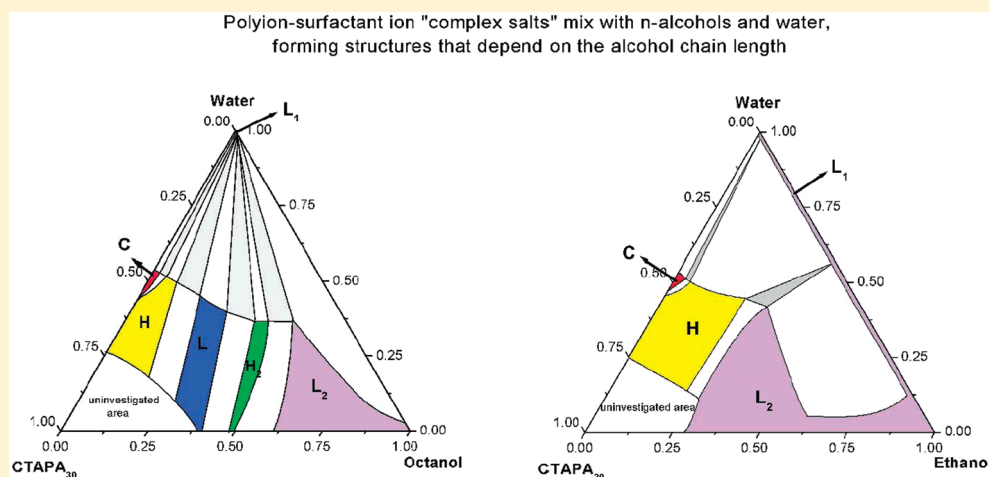


# Self-Assembly of Polyion–Surfactant Ion Complex Salts in Mixtures with Water and *n*-Alcohols

Juliana Silva Bernardes,<sup>†</sup> Lennart Piculell,<sup>‡</sup> and Watson Loh<sup>\*,†</sup><sup>†</sup>Institute of Chemistry, Universidade Estadual de Campinas Campinas (UNICAMP), Caixa Postal 6154, Campinas, SP, Brazil<sup>‡</sup>Physical Chemistry 1, Center for Chemistry and Chemical Engineering, Lund University, P.O. Box 124, S-221 00 Lund, Sweden Supporting Information**ABSTRACT:**

Phase behavior and structural features were investigated for "complex salts", consisting of the cationic hexadecyltrimethylammonium (CTA) surfactant with polyacrylate (PA<sub>*n*</sub>, *n* = 30 or 6000) counterions, mixed with water and different *n*-alcohols (ethanol, butanol, hexanol, octanol, and decanol). The liquid crystalline structures formed were identified by small-angle X-ray scattering measurements, which provided information about the changes in the geometry of the aggregates as functions of the concentration and chain length of the added *n*-alcohol. The obtained results were compared with a previous work on similar ternary mixtures of the same cationic surfactant but with the monomeric bromide counterion, CTABr (Fontell, K.; Khan, A.; Lindström, B.; Maciejewska, D.; Puang-Ngern, S. *Colloid Polym. Sci.*, 1991, 269, 727). In general, the same phases were detected in systems with the complex salts CTAPA<sub>*n*</sub> as in systems with CTABr, but the swelling of the various liquid crystalline phases by water was much more limited in the complex salt systems. An isotropic alcoholic phase was observed with all alcohols and the size of this region of the phase diagram increased for the shorter alcohols, except for ethanol. For mixtures with octanol and ethanol, in particular, the extensions of the disordered isotropic phases were larger for the complex salt with the shorter polyacrylate ions.

## 1. INTRODUCTION

Ionic surfactant molecules display strong association with oppositely charged polyions in water due to electrostatic interactions and give rise to the formation of polyion–surfactant ion complex salts.<sup>1,2</sup> The strong association between the oppositely charged species may lead to an associative phase separation, resulting in one concentrated phase rich in polyions and surfactant ions and one diluted phase containing most of simple counterions and water.<sup>3</sup> The concentrated phase can be a disordered liquid or a liquid crystalline phase (typically cubic, hexagonal, or lamellar) due to the self-assembling properties of surfactant molecules.<sup>4,5</sup>

Associating polymer–surfactant systems are useful in many different situations. The liquid crystalline phases obtained can be used as templates in silica polymerization reactions<sup>6</sup> in drug

delivery systems<sup>7</sup> and in deposition of silicone oil onto hydrophilic surfaces.<sup>8</sup> For all of these applications, it is important to be able to control the phase structure as well the composition and water miscibility of the resulting structure of the associating complex salt, and the most common way to obtain this type of information is by studying the phase behavior of the desired system.<sup>9</sup>

The phase equilibria of these two electrolytes containing a total of four different ions in water is rather complex to study because phases containing mixtures of all four ions in different proportions appear in such mixtures. Thalberg et al.<sup>10</sup> suggested

Received: March 14, 2011

Revised: June 3, 2011

Published: June 08, 2011

a pyramidal phase diagram to represent, specifically, the associative phase separation of mixtures of oppositely charged polyelectrolytes and surfactants in water. To simplify this kind of study, Svensson et al.<sup>1</sup> developed an alternative strategy where the small counterions of the surfactant, the polyelectrolyte, or both were eliminated, and the pure “complex salt”, consisting of surfactant ions with polyions as counterions, was used as a single component. Using this new approach, it is possible to obtain true binary systems when water is mixed with the complex salt and true ternary systems when the complex salt is mixed with water and a third component.<sup>1,2,11,12</sup>

In our research group, the methodology developed by Svensson et al.<sup>1</sup> was used in studies to analyze the effect of adding solvents with different low polarities on the phase behavior of polyion–surfactant ion complex salts in water.<sup>13,14</sup> The main conclusion was that the structure of the liquid crystalline phase assumed by the complex salt is dependent on where the added solvent is located in the surfactant aggregates.<sup>13,14</sup> With xylene, an apolar cosolvent that was mostly located in the aggregate core, a predominance of hexagonal phase was observed, whereas with decanol, which is located at aggregate interface, the phase diagram displays a predominance of lamellar phases.<sup>13,14</sup>

In the present study, we investigate the effect of the n-alcohol carbon chain length on the phase equilibria and structures formed by the complex salts CTAPA<sub>30</sub> and CTAPA<sub>6000</sub> (CTA = hexadecyltrimethyl ammonium; PA = polyacrylate) when mixed with water and alcohol. The effect of the polymeric counterion is illuminated by comparing the results obtained with a prior investigation carried out by Fontell et al.<sup>15</sup> on the same solvent mixtures but employing CTABr as the surfactant. We also compare our results with those of a recent study of complex salts based on DNA in mixtures with water and n-alcohols.<sup>16</sup> A detailed study of the nature of the reverse micelles formed by the complex salts CTAPA<sub>n</sub> in some of the alcohol-rich phases of the present study has been published elsewhere.<sup>17</sup>

## 2. EXPERIMENTAL METHODS

**2.1. Chemicals.** Poly(acrylic acid) (PAA) samples with molar masses of 2000 and 450 000 g mol<sup>-1</sup> (30 and 6000 AA units, respectively) from Sigma were used as received. Hexadecyltrimethylammonium bromide (CTABr) 99% was purchased from Sigma and used without further treatment. Decanol from BDH, octanol from Merck, and hexanol, butanol, and ethanol from Acros, all of the highest purity available, were also used without further treatment. Millipore water with a resistivity of 18 MΩ/cm was used throughout the study.

**2.2. Synthesis of Complex Salts.** Complex salts of CTA<sup>+</sup> with polyacrylate counterions were prepared by titration of the hydroxide form of the surfactant (CTAOH) with the acid forms of the polymers (PAA), according to the procedure developed by Svensson et al.<sup>1</sup> Throughout this text, the complex salts will be named CTAPA<sub>30</sub> and CTAPA<sub>6000</sub>, where 30 and 6000 refer to the average degrees of polymerization of the polyions.

**2.3. Sample Preparation.** Appropriate amounts of complex salt, water, and n-alcohol were weighed into glass tubes. After mixing with a Vortex vibrator, the tubes were flame-sealed. Sample mixing continued in a centrifuge at 25 °C where the tubes were turned end-over-end every 30 min for several times. The samples were left to equilibrate at 25 °C for at least 1 month. No differences were observed when older samples of the same compositions were investigated.

**2.4. Methods.** The samples were investigated by visual inspection in normal light and between crossed polarizers to detect optically anisotropic phases (lamellar, hexagonal, and reverse hexagonal).

SAXS measurements were performed in the SAXS beamline (D02A) of the Brazilian Synchrotron Laboratory (LNLS) at Campinas, Brazil. The experimental setup involved the use of X-rays at the wavelength of 1.488 Å and a sample-to-detector distance of 591.2 mm. For these experiments, a sample cell with mica windows was used with temperature control. (All measurements were made at 25 °C.) Typical acquisition times were ca. 5 min. The collected data were treated using the software Fit2D, which allows the integration of detector images.<sup>18</sup>

## 3. RESULTS

**3.1. Strategy of Investigating the Phase Diagrams.** Ternary systems of the two complex salts (C<sub>16</sub>TAPA<sub>30</sub>, C<sub>16</sub>TAPA<sub>6000</sub>) with water and n-alcohol (ethanol, butanol, hexanol, octanol, and decanol) were analyzed and are represented in conventional triangular phase diagrams, as shown in Figures 1 and 2. The general approach used to investigate all phase diagrams was to focus on dilution lines, referred to as alcohol and water dilution lines. The analyzed n-alcohol dilution line (indicated in Figure 1a) starts with a binary mixture of ca. 30 wt % of complex salt and 70 wt % of water, which contains two-phase samples of either a cubic phase (for CTAPA<sub>30</sub>) or a hexagonal phase (for CTAPA<sub>6000</sub>) in equilibrium with almost pure water.<sup>2</sup>

Along such a dilution line, the effects caused by the addition of various alcohols can be followed. Different water dilution lines were also investigated in the concentrated region of the phase diagrams to elucidate specific features of each system. All boundaries indicated in Figures 1 and 2 as solid lines were quantitatively determined by investigating samples close to the boundaries. Dotted lines define boundaries between regions that were not directly observed with the prepared samples and hence represent estimated positions.

The solubilities of the two complex salts in the n-alcohols were not quantitatively measured in this work, but estimates can be obtained at the n-alcohol–complex salt axis in the ternary phase diagrams shown in Figures 1 and 2. For both complex salts, the solubility of CTAPA<sub>n</sub> increases as the n-alcohol alkyl chain length decreases. The estimated solubilities in decanol, octanol, hexanol, butanol, and ethanol are, respectively, 10, 40, 60, 65, and 70 wt % for CTAPA<sub>30</sub> and 8.5, 20, 40, 65, and 50 wt % for CTAPA<sub>6000</sub>.

**3.2. Decanolic System.** Phase diagrams of decanolic systems were determined and described in detail in a previous study<sup>14</sup> but are included here for the sake of completeness. In brief, at the starting point of the alcohol dilution line (binary mixture of water + complex salt), the systems display two phases in equilibrium: a bottom isotropic liquid phase (L<sub>1</sub>) and a top liquid crystalline phase. For CTAPA<sub>30</sub>, the liquid crystalline phase is a Pm3n cubic phase, and for CTAPA<sub>6000</sub>, the top phase is an anisotropic hexagonal phase. Along the alcohol dilution line, the CTAPA<sub>30</sub> complex salt assumed three liquid crystalline structures: cubic (C), hexagonal (H), and lamellar (L), whereas the CTAPA<sub>6000</sub> complex salt assumed only hexagonal and lamellar structures. The phase transitions from cubic to hexagonal and from hexagonal to lamellar were detected when small amounts of decanol were added to the systems, as shown in Figures 1A and 2A, which indicate that decanol acts effectively as a cosurfactant, favoring structures with low curvature. At the end of the alcohol dilution line, a small region with an alcoholic solution (L<sub>2</sub>) was detected for both complex salt systems.

**3.3. Octanolic System.** The phase diagrams of octanolic systems, shown in Figures 1B and 2B, present two liquid isotropic phases: one composed of almost pure water (L<sub>1</sub>) and the other

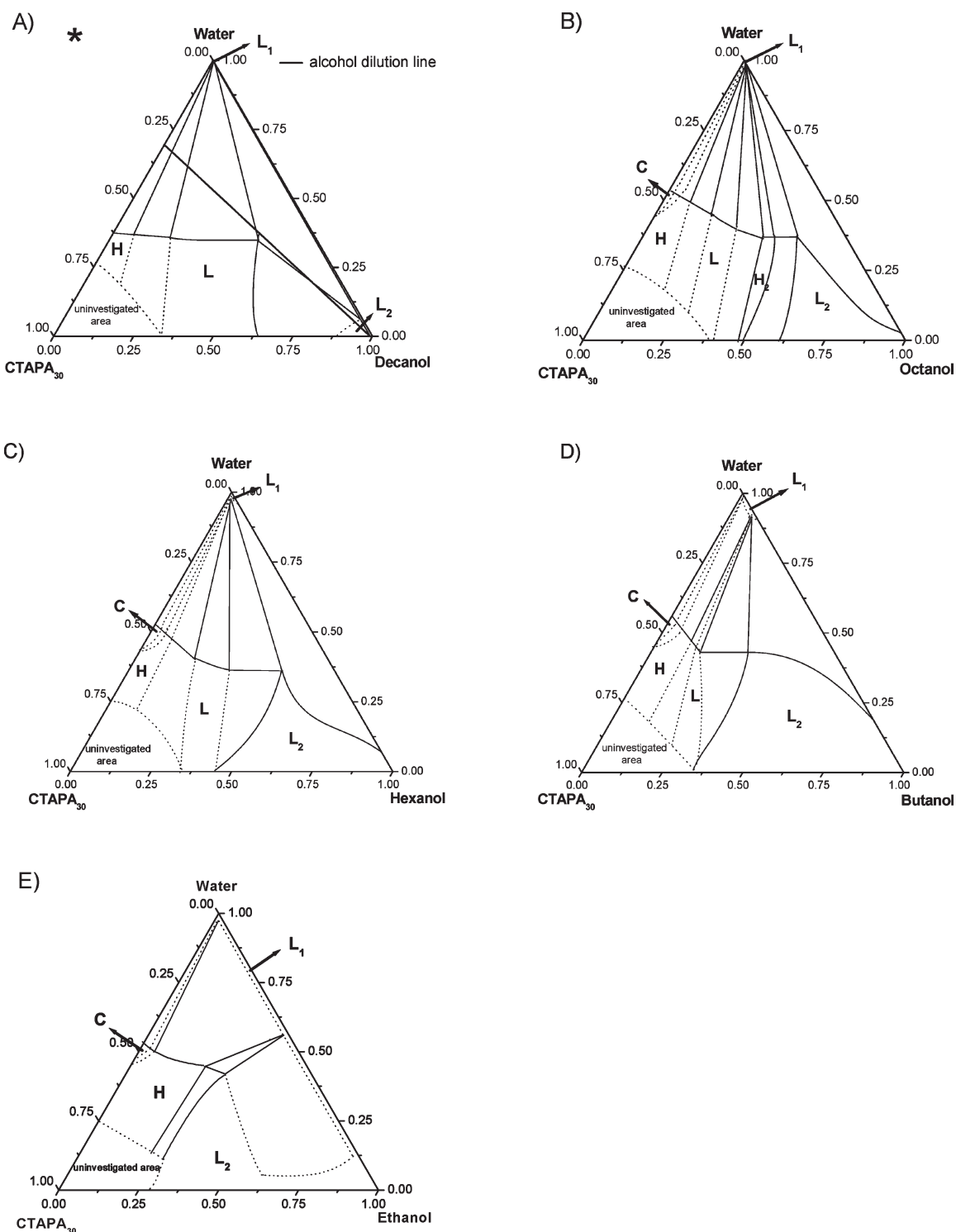


**Figure 1.** Phase diagram of the *n*-alcohol/water/CTAPA<sub>30</sub> systems at 25 °C: (A) decanol,<sup>14</sup> (B) octanol, (C) hexanol, (D) butanol, and (E) ethanol. Codes for phases: L<sub>1</sub>, aqueous isotropic solution; C, cubic; H, hexagonal; L, lamellar; H<sub>2</sub>, reverse hexagonal; L<sub>2</sub>, alcoholic isotropic solution. The alcohol dilution line used for comparison among different systems is indicated in part A.

one located close to the octanol rich-corner (L<sub>2</sub>). Throughout the phase diagram, the complex salt CTAPA<sub>30</sub> self-assembles into four different liquid crystalline structures: cubic (C), hexagonal (H), lamellar (L), and reverse hexagonal (H<sub>2</sub>). With the longer complex salt CTAPA<sub>6000</sub>, the cubic phase was not detected, being absent also in the binary mixture: complex salt + water.<sup>2</sup>

Upon addition of octanol to the CTAPA<sub>30</sub> + water mixture, the cubic phase disappears, even in samples prepared close to the complex salt–water axis. However, a narrow biphasic region with C + L<sub>1</sub> and a three-phase region with C + H + L<sub>1</sub> are represented in the ternary phase diagram, as required by the Gibbs phase rule.

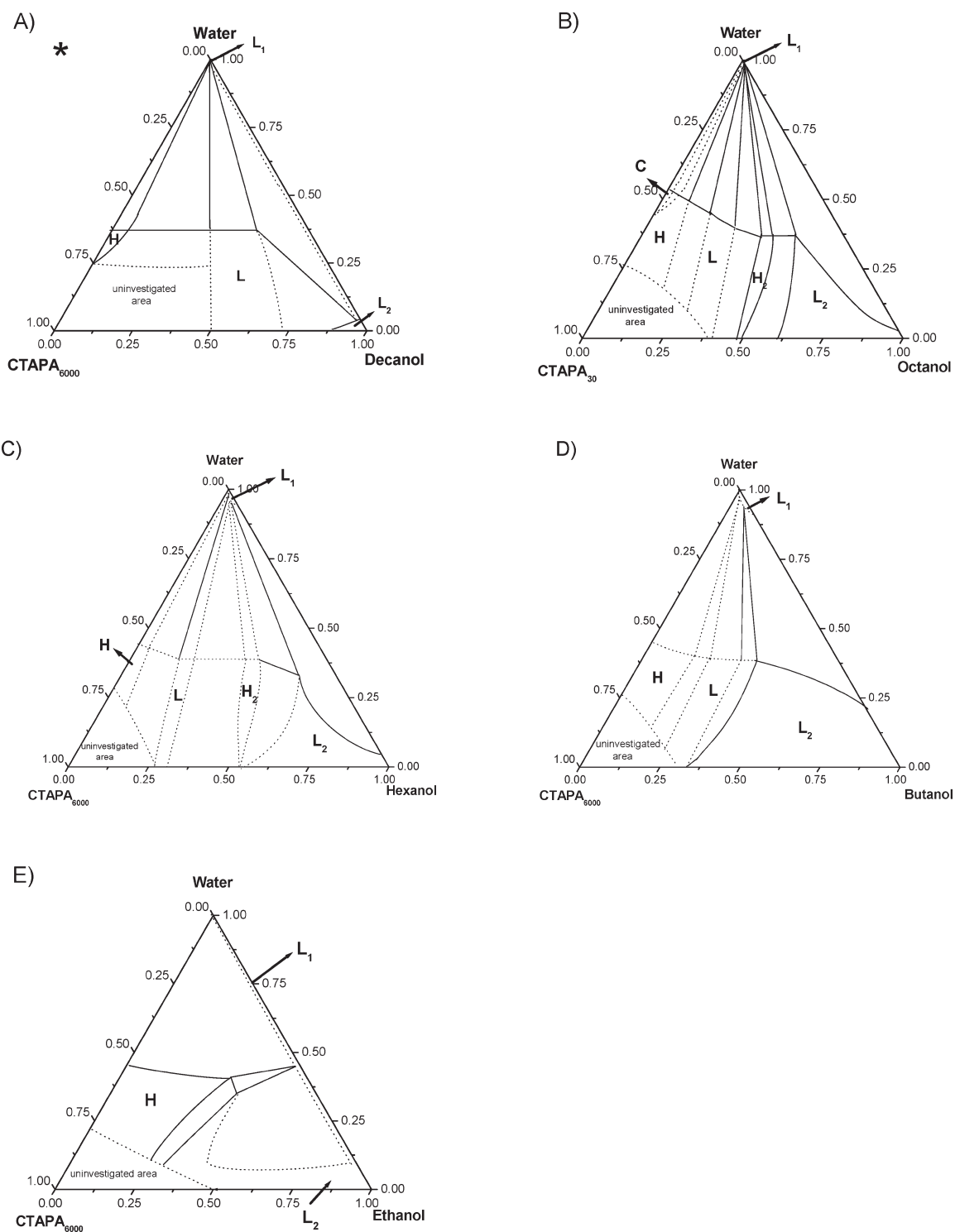


**Figure 2.** Phase diagram of the *n*-alcohol/water/CTAPA<sub>6000</sub> systems at 25 °C: (A) decanol,<sup>14</sup> (B) octanol, (C) hexanol, (D) butanol, and (E) ethanol. Codes for phases: L<sub>1</sub>, aqueous isotropic solution; H, hexagonal; L, lamellar; H<sub>2</sub>, reverse hexagonal; L<sub>2</sub>, alcoholic isotropic solution.

Along the alcohol dilution line, the octanol molecules must be quantitatively incorporated into the surfactant aggregates because of low water solubility of octanol (0.064 wt %).<sup>19,20</sup> Thus, the L<sub>1</sub> phase, present in the CTAPA<sub>30</sub> and CTAPA<sub>6000</sub> systems, can be assumed to be almost pure water because the complex salts do not dissolve in water either.<sup>2</sup>

At low octanol content, both systems present a normal hexagonal phase in equilibrium with excess of water (H + L<sub>1</sub>). The normal hexagonal phase, whose SAXS peaks appear at relative positions 1, 3<sup>1/2</sup>, 2, presents cell parameter of 51 Å for CTAPA<sub>30</sub> and 50 Å for CTAPA<sub>6000</sub>. The hydrophobic radius of the cylinders, calculated following Kunieda et al.,<sup>21,22</sup> is ca. 15 Å for both systems. The biphasic region (H + L<sub>1</sub>) persists until

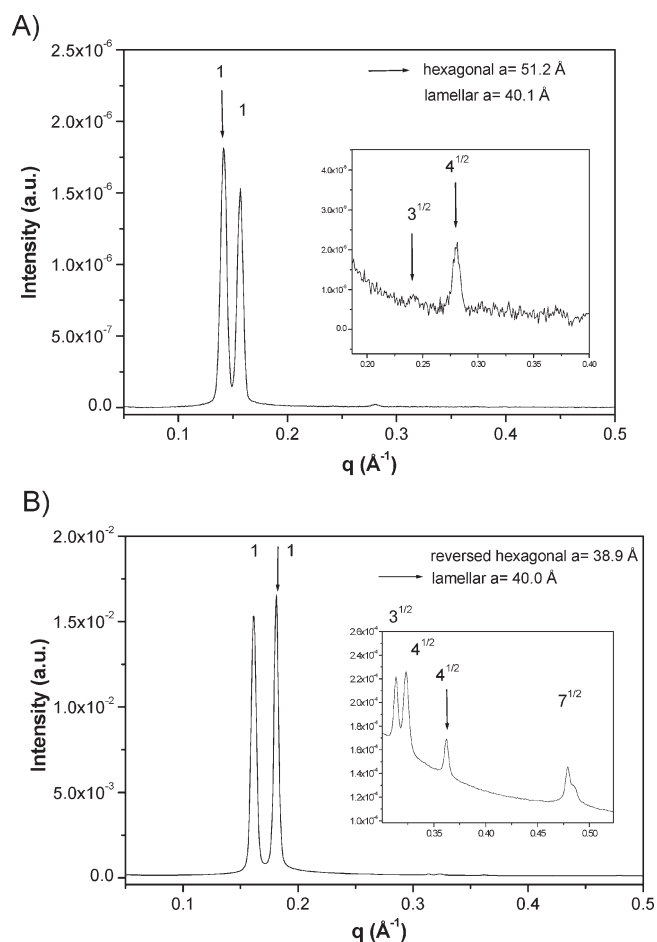


**Figure 3.** SAXS spectra of samples contained in regions (A) H + L (composition: 7 wt % of octanol, 69 wt % of water and 24 wt % of C<sub>16</sub>TAPA<sub>30</sub>) and (B) L + H<sub>2</sub> (composition: 38 wt % of octanol, 34 wt % of water, and 28 wt % of CTAPA<sub>30</sub>).

6 wt % of octanol for CTAPA<sub>30</sub> and 3 wt % of octanol for CTAPA<sub>6000</sub>, where a three-phase region containing hexagonal + lamellar + L<sub>1</sub> phases is reached. A SAXS spectrum of the mixture (lamellar + hexagonal) is shown in Figure 3A. Within this region, the hydrophobic radius and bilayer thickness calculated for hexagonal and lamellar phases are, respectively, 18 and 19 Å for CTAPA<sub>30</sub> and 18 and 18 Å for CTAPA<sub>6000</sub>.

When the octanol mass fraction reaches ~13 wt % for CTAPA<sub>30</sub> and 9 wt % for CTAPA<sub>6000</sub>, the systems assume a biphasic region with a lamellar phase in equilibrium with L<sub>1</sub> (L + L<sub>1</sub>). This two-phase region extends up to 20 wt % of octanol for CTAPA<sub>30</sub> and up to 23 wt % for CTAPA<sub>6000</sub>. The lamellar phase displays SAXS peaks at relative positions 1, 2, and 3 with a repeated distance ranging from 41 to 44 Å for CTAPA<sub>30</sub> and from 43 to 44 Å for CTAPA<sub>6000</sub>. The bilayer thickness calculated within this region varies from 16 to 19 Å for the smaller complex salt and from 18 to 20 Å for the longer complex salt.

As more alcohol is added to the mixture, a further three-phase region with lamellar + reverse hexagonal + L<sub>1</sub> phases appears. The SAXS spectra of the mixture (lamellar + reverse hexagonal) are shown in Figure 3B. This three-phase region remains until 30 wt % of octanol for CTAPA<sub>30</sub> and until 36 wt % of octanol for CTAPA<sub>6000</sub>, and it is followed by a biphasic region with a reverse hexagonal phase (H<sub>2</sub>) in equilibrium with L<sub>1</sub>. SAXS spectra of the

reverse hexagonal phase have peaks at the same relative positions as the normal hexagonal phase; the cell parameter within the biphasic region is ca. 44 Å for CTAPA<sub>30</sub>. The corresponding internal radius of the cylinders is 15 Å.

At around 35 and 42 wt % of octanol for CTAPA<sub>30</sub> and CTAPA<sub>6000</sub>, respectively, an upper isotropic liquid phase (L<sub>2</sub> phase) appears in equilibrium with the L<sub>1</sub> and reverse hexagonal phases. This three-phase region (H<sub>2</sub> + L<sub>1</sub> + L<sub>2</sub>) extends up to 48 wt % of octanol for CTAPA<sub>30</sub> and up to 93 wt % for CTAPA<sub>6000</sub>.

At higher alcohol contents, from 48 to 94 wt % for CTAPA<sub>30</sub> and just close to the water–octanol axis for CTAPA<sub>6000</sub>, the mixtures display a biphasic region with two isotropic phase in equilibrium (L<sub>1</sub> + L<sub>2</sub>). This L<sub>2</sub> phase was extensively studied in a parallel work,<sup>17</sup> and the results revealed that the alcoholic solution is composed of reverse elongated micelles with a hydrophilic core that contains water, polyanion, and the surfactant head-groups and a corona with the surfactant and n-alcohol tails.

Finally, at the end of the alcohol dilution line, a one-phase region containing only the alcoholic isotropic phase (L<sub>2</sub> phase) is observed for the octanol systems.

**3.4. Hexanolic System.** The phase diagrams with hexanol, shown in Figures 1C and 2C, are quite similar to those obtained for octanol. The principal difference is related to the reverse hexagonal phase, which was not detected for the complex salt with the shorter polyion. Increasing the alcohol content along the dilution line, the hexanol molecules must be preferentially incorporated in the liquid crystalline phases because of their low water solubility (0.7 wt %).<sup>19,20</sup>

The regions: cubic + L<sub>1</sub>, cubic + hexagonal + L<sub>1</sub>, hexagonal + L<sub>1</sub> for CTAPA<sub>30</sub>, and hexagonal + L<sub>1</sub> for CTAPA<sub>6000</sub> are drawn as dashed lines because they were not detected during experiments. At ~5 wt % of hexanol for CTAPA<sub>30</sub> and 2 wt % of hexanol for CTAPA<sub>6000</sub>, the ternary mixtures display a three-phase region with hexagonal + lamellar + L<sub>1</sub> phases in equilibrium. The cell parameters of the hexagonal and lamellar liquid crystalline phases in this region are, respectively, 60 and 45 Å for CTAPA<sub>30</sub> and 62 and 46 Å for CTAPA<sub>6000</sub>. On increasing the alcohol content to 11 wt % for CTAPA<sub>30</sub> and to 9 wt % for CTAPA<sub>6000</sub>, a biphasic region with lamellae in equilibrium with L<sub>1</sub> is reached. The cell parameter and the corresponding value of bilayer thickness within the biphasic area are 46 and 22 Å for CTAPA<sub>30</sub> and 46 and 22 Å for CTAPA<sub>6000</sub>. In the CTAPA<sub>30</sub> system, the cell parameter and the bilayer thickness range from 44 to 46 Å and from 23 to 25 Å, respectively.

At slightly higher hexanol concentration (13 wt %), the system with CTAPA<sub>6000</sub> displays another three-phase region: lamellar + reverse hexagonal + L<sub>1</sub>, as observed in systems with octanol. This three-phase region is maintained until 29 wt % of hexanol, and it is followed by a biphasic region with a reverse hexagonal phase (H<sub>2</sub>) in equilibrium with L<sub>1</sub>. The cell parameter and internal radius of the cylinders for the reverse phase are 47 and 16 Å, respectively.

When more hexanol is added to the system, at 22 wt % for CTAPA<sub>30</sub> and 35 wt % for CTAPA<sub>6000</sub>, an upper isotropic liquid phase (L<sub>2</sub> phase) appears in equilibrium with L<sub>1</sub> + lamellar for CTAPA<sub>30</sub> and in equilibrium with L<sub>1</sub> + reverse hexagonal for CTAPA<sub>6000</sub>. The three-phase region remains until 47 wt % of alcohol for the smaller complex salt and until 55 wt % of alcohol for the longer complex salt. The next region detected along the alcohol dilution line is a biphasic region with two isotropic liquids in equilibrium (L<sub>1</sub> + L<sub>2</sub>). At alcohol concentrations above

82 wt % for CTAPA<sub>30</sub> and 91 wt % for CTAPA<sub>6000</sub>, the ternary mixtures present just one single phase ( $L_2$ ).

**3.5. Butanolic System.** The ternary phase diagram with butanol for CTAPA<sub>30</sub>, shown in Figure 1D, has the same regions as detected in the hexanol system; the differences observed are just related to the positions of the borders. An additional difference between the hexanolic and the butanolic systems was found for CTAPA<sub>6000</sub> (Figure 2D) because the reverse hexagonal phase was not detected with butanol.

On increasing the alcohol content along the dilution line, the butanol molecules should go to both the liquid crystalline phase and the aqueous isotropic phase ( $L_1$ ) because butanol molecules have a significant solubility in water (8 wt %).<sup>19,20</sup> Therefore, for this system, we cannot assume that the n-alcohol quantitatively ends up in the liquid crystalline phase. Moreover, because the  $L_1$  phase should contain some butanol, it could also dissolve some complex salt. This has not been investigated here.

At low butanol content for CTAPA<sub>30</sub> system, some regions were not detected (cubic +  $L_1$  and cubic + hexagonal +  $L_1$ ) during the experiments because they represent narrow regions, which makes difficult to prepare samples with the exact compositions that fit in these regions. Nevertheless, they are represented by dashed lines because their presence is required by the Gibbs phase rule.

For both complex salt systems, a region with a hexagonal phase in equilibrium with  $L_1$  appears in the beginning of the alcohol dilution line. This region extends until 9 wt % of butanol for CTAPA<sub>30</sub> and until 10 wt % of butanol for CTAPA<sub>6000</sub>. The cell parameter and the hydrophobic radius calculated for the hexagonal phase are, respectively, 59 and 19 Å for CTAPA<sub>30</sub> and 60 and 21 Å for CTAPA<sub>6000</sub>.

As more butanol is added to the system, the complex salts assume a lamellar liquid crystalline phase. The hexagonal-to-lamellar phase transition starts in a narrow three-phase region containing hexagonal + lamellar +  $L_1$  phases, which is followed by biphasic region with lamellar +  $L_1$  phases.

At ~12 wt % of butanol for CTAPA<sub>30</sub> and 25 wt % of butanol for CTAPA<sub>6000</sub>, an alcoholic isotropic phase ( $L_2$ ) appears in equilibrium with the lamellar and  $L_1$  phases. The three-phase region extends up to 25 wt % of alcohol for the complex salt with the shorter polyion and up to 30 wt % of alcohol for CTAPA<sub>6000</sub>. The cell parameter and the bilayer thickness for the lamellar phase within this three-phase region are, respectively, 44 and 19 Å for CTAPA<sub>30</sub> and 44 and 23 Å for CTAPA<sub>6000</sub>. Upon further increasing the butanol content, the ternary systems displays two isotropic  $L_1$  and  $L_2$  phases in equilibrium.

Above 41 wt % of butanol for CTAPA<sub>30</sub> and 51 wt % of butanol for CTAPA<sub>6000</sub>, the system reaches a large one-phase region containing an alcoholic isotropic phase, which is composed of reverse elongated micelles, as described in more detail in another publication.<sup>17</sup>

**3.6. Ethanolic System.** The ternary phase diagrams with ethanol are shown in Figures 1E and 2E. These phase diagrams have different features than those observed with the higher alcohols. For example, the lamellar liquid crystalline phase, which is present in all of the other systems, was not detected with ethanol.

On increasing the alcohol content along the dilution line, the ethanol molecules, as in butanol system, should be incorporated both in the liquid crystalline phase and in the aqueous isotropic phase ( $L_1$ ) because of complete miscibility of water and ethanol. At low ethanol concentration (2 wt %), a narrow biphasic region with cubic +  $L_1$  phases was detected for CTAPA<sub>30</sub>. The SAXS spectrum of the  $Pm\bar{3}n$  cubic phase is represented in Figure 4.

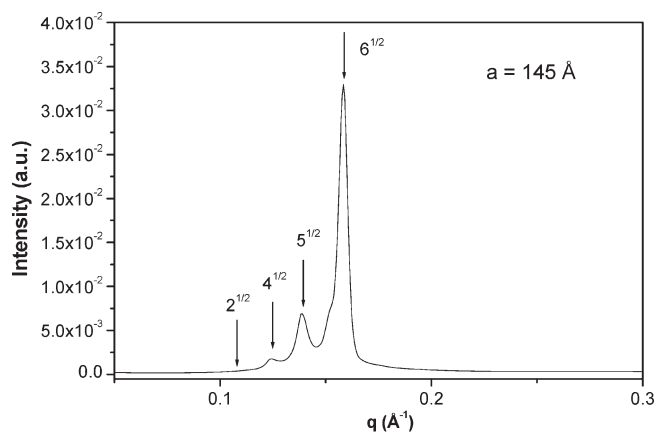


**Figure 4.** SAXS spectra of sample contained in region C +  $L_1$  (composition: 4 wt % of ethanol, 69 wt % of water, and 27 wt % of CTAPA<sub>30</sub>).

The cell parameter calculated for this phase is 145 Å, which is 40 Å larger than that obtained for the binary complex salt + water system.<sup>2</sup> As ~3 wt % ethanol was added to the system, a cubic-to-hexagonal phase transition was observed. The three-phase region cubic + hexagonal +  $L_1$  was not detected during the experiment because it represents a narrow area in the phase diagram, being difficult to prepare a sample with the exact composition that fits this region. However it is represented in the phase diagram for consistency with the Gibbs phase rule.

The biphasic region containing  $L_1$  + hexagonal phases extends from 5 to 30 wt % of ethanol for CTAPA<sub>30</sub> and from 0 to 40 wt % of ethanol for CTAPA<sub>6000</sub>. The cell parameter of the liquid crystalline phase varies from 44 to 46 Å for the shorter polyion and from 40 to 44 Å for the longer polyion. In these cases, the cylinder dimensions could not be estimated because it is difficult to determine the exact amount of ethanol present in the aqueous and micellar phases.

As more ethanol was added to the system, a narrow three-phase region containing  $L_1$  + hexagonal liquid crystalline phase and a top viscous isotropic phase appeared for both systems. The latter viscous phase ( $L_2$ ) displayed optical birefringence when sheared between crossed polarizers. A SAXS spectrum of the  $L_2$  phase presents only a single correlation peak and is shown in Figure 5. According to our previous results for mixtures with butanol, hexanol, and octanol,<sup>17</sup> the  $L_2$  phase is composed of reverse polyion–surfactant ion aggregates, where a fraction of the surfactant counterions may be dissociated from the central polyion, dissolved in the alcohol medium. We conclude that at a certain critical content of ethanol the hydrophobically associated normal surfactant aggregates, which exist in the wide water-rich normal hexagonal phase of the phase diagram, dissolve into electrostatically stabilized reverse aggregates because of the lower cohesive energy of ethanol compared with water.

A large biphasic region with two isotropic phases in equilibrium was detected from 34 to 85 wt % of ethanol for CTAPA<sub>30</sub> and from 45 to 87 wt % for CTAPA<sub>6000</sub>. At the end of ethanol dilution line, the ternary mixtures enter the dilute branch of the  $L_2$  phase.

## 4. DISCUSSION

The effect of adding n-alcohol to the system containing water + complex salt was analyzed along an alcohol dilution line, as

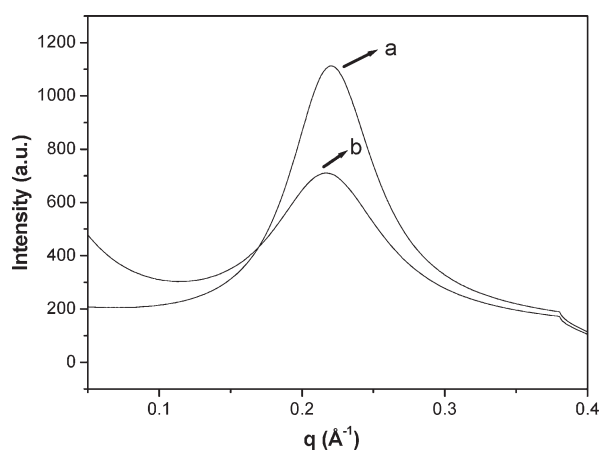


**Figure 5.** SAXS spectra of samples contained in region  $L_2$ : (a) composition: 35 wt % of ethanol, 17 wt % of water, and 48 wt % of  $C_{16}TAPA_{30}$ , and cell parameter = 28.5 Å; (b) composition: 55 wt % of ethanol, 15 wt % of water, and 30 wt % of  $CTAPA_{30}$  and cell parameter = 28.8 Å.

described in the previous section. Different trends were verified for the ternary phase diagrams studied. First of all, it was observed that as the *n*-alcohol chain length decreases, the regions occupied by the liquid crystalline phases generally decrease, whereas the areas occupied by liquid isotropic phases ( $L_1$  and  $L_2$ ) as well as the complex salt solubility increase. A second important finding is that the sequence of the phases, along this dilution line, is similar to that obtained for  $CTABr^{15}$  for all studied alcohols. Thus, the self-assembled structures seem to be determined by the hydrocarbon chain lengths of the surfactant ion and of the alcohol.

**Cosurfactant and Cosolvent Effects.** Different trends observed along the *n*-alcohol dilution line are related to two extreme effects that may be caused by *n*-alcohol molecules, namely, a cosurfactant effect and a cosolvent effect. Decanol acts purely as a cosurfactant and dissolves among the  $CTA^+$  molecules with the hydroxyl groups located at the aggregate interface. This leads to an increase in the critical packing parameter,<sup>23</sup> favoring the formation of structures with low curvature both for  $CTAPA_n^{14}$  and  $CTABr^{15}$  systems.

For intermediate alcohols (butanol, hexanol, and octanol), the transitions from cubic to hexagonal and from hexagonal to lamellar phases were also detected at low alcohol content. (See Table 1.) The data in Table 1 confirm that the alcohols with longer carbon chains are more effective in promoting transition toward liquid crystalline phases with lower curvature. When octanol or hexanol are added to  $CTAPA_{30}$  + water systems, the area per ionic surfactant headgroup for the lamellar phase increases from 68 to 147 or from 73 to 101 Å<sup>2</sup>, respectively. This behavior indicates that the *n*-alcohol molecules dissolve as cosurfactant molecules between surfactant molecules within the aggregates, independently of their alkyl chain length, which leads to a change in the liquid crystalline structure as the *n*-alcohol concentration increases. For butanol systems, these transitions occurred at slightly higher alcohol content, probably because only a fraction of the alcohol molecules is incorporated into the aggregates. Hence, a higher total concentration of butanol is necessary to cause the same effect as observed for octanol or hexanol.

Besides the cosurfactant effect, the intermediate alcohols also may act as cosolvents, depending on their carbon chain length. Upon varying the alcohol from octanol to butanol, the miscibility

**Table 1.** *N*-Alcohol/Surfactant Ion ( $CTA^+$ ) Weight Ratio at the Different Phase Transitions along the Alcohol Dilution Line Represented in Figure 1

<i>n</i> -alcohol	cubic–hexagonal	hexagonal–lamellar	lamellar–reverse
			hexagonal
decanol <sup>14</sup>	0.05	0.15	
octanol	0.08	0.27	1.1
hexanol	0.08	0.25	

with water and the tendency to form the  $L_2$  phase increase. The tendency to assemble into reverse liquid crystalline structures, such as reverse hexagonal phase, decreases. These findings reveal that the “solvent quality” for the long reverse micelles rises with decreasing alcohol chain length. The tendency to form  $L_2$  phase may be related to changes in the entropy of mixing in these mixtures. Jönsson et al.<sup>24</sup> argued that the entropy term depends on the size of the molecules in the bulk medium, and for alcohols, this means that the term becomes more important for shorter alcohols, with small molecules mixing better with the surfactant palisade layer of the reverse aggregate, favoring the formation of disordered phases.

A detailed investigation of the nature of the  $L_2$  phase was the subject of a previous publication,<sup>17</sup> where it was concluded that these aggregates are composed of polyion chains decorated by the surfactant molecules with some water dissolved in its core, behaving like reverse micelles with a spine.

The balance of the tendency to form reverse hexagonal and disorder micellar phases ( $H_2$  and  $L_2$ ) can be used as an estimate of solvent quality for the surfactant or complex salt. Octanol seems to be a “marginal solvent”; it readily dissolves  $CTABr$  micelles<sup>15</sup> and small reverse micelles of  $CTAPA_{30}$ . However, the long reverse micelles of  $CTAPA_{6000}$  do not dissolve well in octanol, resulting in a small  $L_2$  phase region in the phase diagram (Figure 2B). Interestingly, preliminary results on temperature effects on these phase equilibria demonstrated that a reverse  $H_2$  phase appears in the  $CTAPA_{30}$ /decanol/water system at 40 °C, whereas this structure is absent at 25 °C. Following the reasoning above, this finding suggests that decanol becomes a better solvent for the complex salts as the temperature is raised.<sup>14,25</sup>

In the case of hexanol and butanol, a large  $L_2$  phase region is present independently of the length of the counter-polyion, which indicates that these *n*-alcohols are good solvents for the complex salts. In polymer language, hexanol, and butanol are better-than- $\theta$  solvents, whereas octanol should be considered as a worse-than- $\theta$  solvent.

For ethanolic systems with  $CTAPA_n$  and  $CTABr^{15}$  the cosurfactant effect can be ruled out: the ternary phase diagrams are rather different from those obtained with the longer alcohols. A predominance of the normal hexagonal phase and an absence of a lamellar phase are evident. Furthermore, at high ethanol concentration, the complex salt dissolves, forming the  $L_2$  phase. All of these trends classify ethanol purely as a solvent, because it mainly occupies the continuous medium.

When comparing the extension of the  $L_2$  region for  $CTAPA_n$  systems, one observes that it is larger for butanol than for ethanol. This fact can be understood by taking into account the water miscibility with butanol and ethanol. In the butanol systems, the water molecules predominantly enter the interior of the mixed micelles, and in this way, the solvent quality of the continuous butanol phase remains mostly unchanged along a water dilution

line. In contrast, in ethanol systems, the water molecules dissolve mainly in the ethanol continuous phase because of their complete miscibility, which changes the solvent quality, promoting a liquid–liquid phase separation of reverse polyion–surfactant ion aggregates along a miscibility gap.

**Monomeric and Polymeric Counterions.** The comparison between this work and the similar investigation conducted by Fontell et al.<sup>15</sup> on the phase behavior and structure analyses of CTABr in water with a range of different *n*-alcohols can provide insight into the polyanion effect.

Along the alcohol dilution line, the same trends were observed for systems with both monomeric bromide and polymeric polyacrylate counterions. For each of the longer *n*-alcohols: decanol, octanol, hexanol, and butanol, CTABr and CTAPA<sub>*n*</sub> displayed almost the same liquid crystalline structures in the ternary mixtures with water and *n*-alcohol. The only difference was the presence of inverted phases with CTABr in decanol, which was not observed with CTAPA<sub>*n*</sub>. In ethanolic systems, the hexagonal structure was the only liquid crystalline structure encountered for both the complex salts CTAPA<sub>*n*</sub> and the surfactant CTABr. This evidence allows us to conclude that the aggregate geometry in these ternary systems for a given surfactant ion is mainly determined by the alkyl chain length of the *n*-alcohol.

An important difference verified in these systems is related to the swelling of the liquid crystalline phases by water. With polymeric counterions, the lamellar phase for decanol, octanol, and hexanol incorporates ~40 wt % of water, and with bromide as counterion, the lamellar structure absorbed an almost unlimited amount of water. These results confirm the existence of greater attractive forces between the planar aggregates due mainly to the polyanionic bridging between the aggregates.<sup>26</sup> In the case of the monomeric counterions (CTABr + *n*-alcohol), a high swelling is the result of long-range repulsive force. Svensson et al.<sup>26</sup> showed that the phase diagram for CTA<sup>+</sup> micelles with mixed polymer and monomeric counterions reveals that the micelle–micelle interaction changes from repulsive, when the simple counterions dominate, to strongly attractive, when the polymeric counterions dominate. This trend was supported by computer simulations, which also showed that the dominating attractive term is polyion bridging. It is interesting to note that no major differences were observed, comparing both the phase behavior and the structural parameter of liquid crystalline phases formed with the long and short complex salts, indicating that this effect is already predominant for a polyanion with 30 repeating units.<sup>14</sup> In fact, Norrman et al.<sup>27</sup> showed that using di-, tri-, or tetravalent carboxylates as CTA<sup>+</sup> counterions, the strong attraction between the planar aggregates is already well-established.

The previous study of the ternary system of CTABr + water + butanol<sup>15</sup> found a large one-phase region extending from the water-rich to the butanol-rich corner. Although Fontell and co-workers did not investigate the nature of this phase, it is reasonable to assume that close to the water and butanol corners, CTABr assembles as normal (L<sub>1</sub>) and reverse (L<sub>2</sub>) micelles, respectively. At moderate concentrations of butanol, the observation of a homogeneous isotropic phase may be understood as the formation of a CTABr solution or a bicontinuous phase, but the details provided do not allow discrimination of which one is occurring. More recently, a similar study<sup>28</sup> with gemini cationic surfactant in water and butanol proposed the formation of a bicontinuous phase in this same area of their phase diagrams, although no direct evidence was reported to support this claim. Results from the present investigation show that the addition of

complex salt CTAPA<sub>*n*</sub> to a biphasic water–butanol mixture leads to the partitioning of the complex salt entirely to the butanolic L<sub>2</sub> phase, without a merging of the butanol- and water-rich phases on further addition of complex salt. The failure in forming a continuous complex salt solution in water/butanol mixtures may be ascribed to a stronger attraction between the surfactant molecules with the polymeric counterions and hence reduced solubility due to the presence of the polymeric counterion.

In the phase diagram for the ternary system CTABr + water + ethanol,<sup>15</sup> a large one-phase region starting from the water–ethanol corner occupies ca. 70 wt % of the phase diagram. In this region, complete miscibility among the three components occurs, producing an isotropic solution. For CTAPA<sub>*n*</sub> systems, the addition of complex salts to the mixture of water + ethanol leads to phase separation in samples with less than ca. 75 wt % of ethanol. Again, the failure in forming a large extension of the complex salt solution may be ascribed to a stronger attraction between the polyion–surfactant ion aggregates. In fact, the latter reverse aggregates show the classical trend for polymers in a poor solvent in that the miscibility gap increases with increasing degree of polymerization of the polymer.

An L<sub>2</sub> phase was also detected in systems where CTABr was mixed with decanol, octanol, or hexanol and water.<sup>15</sup> In these systems, some water (approximately a fixed mass of water molecules per unit mass of surfactant) was required to form the L<sub>2</sub> phase. In contrast, for the polymeric counterion, the alcoholic solution was found already for the driest systems investigated, where the water content was determined by the finite content of water in the freeze-dried complex salts.

A recent investigation by Leal et al.<sup>16</sup> showed the effect of *n*-alcohol addition in aqueous systems composed of a complex salt of a cationic surfactant (dodecyltrimethylammonium, DTA) with DNA as counterion. The obtained results showed several of the trends observed in the present work: The longer *n*-alcohol acted as cosurfactant favoring lamellar structures, and, as the *n*-alcohol chain length decreased, the disordered phases became more favorable and occupied a larger area of the phase diagram. The solubility of the complex DNA salt in pure alcohol also increased with decreasing alkyl chain length of the alcohol, although the effect was not as large as was found here for CTAPA<sub>*n*</sub>. However, there were also distinct differences because the one-phase areas were generally quite narrow in the DTADNA system and were separated from neighboring one-phase areas by large miscibility gaps. Two particular notable differences were the low maximum water uptake in the L<sub>2</sub> phases of DTADNA with hexanol and butanol and the absence of a large normal hexagonal phase in the mixtures with ethanol. Thus, the interesting analogies with the mixtures containing the simple CTABr surfactant, which we found and highlighted here for the CTAPA<sub>*n*</sub> systems, were largely absent for the systems containing DTADNA.

The phase behavior of systems containing DTAPA<sub>*n*</sub> complex salts has been previously studied<sup>2,29</sup> but not for mixtures with alcohols. Overall, the studied DTAPA<sub>*n*</sub> systems showed large similarities to the corresponding CTAPA<sub>*n*</sub> systems, although the shorter surfactant tail generally gave a larger water uptake and a shift of the hexagonal phase toward higher surfactant ion concentrations. The similarities between DTAPA and CTAPA systems suggest that most of the differences between DTADNA and CTAPA<sub>*n*</sub> in their mixtures with long-chain alcohols and water, are due to the differences between the DNA and PA polyions.



## 5. CONCLUSIONS

In this work, the effect of adding alcohols with different alkyl chain lengths in systems composed of complex salt CTAPA<sub>n</sub> and water was analyzed. The packing of the surfactant molecules was strongly affected by the alcohols; decanol, octanol, hexanol, and butanol all favored structures with lower curvature, such as the lamellar phase. The region occupied by the alcoholic isotropic phase (L<sub>2</sub> phase) increased as the n-alcohol chain length decreased, which was ascribed to a better miscibility of the shorter chain alcohols with the surfactant chains in the palisade layer of the reverse micelles. In the mixtures with ethanol, the addition of water decreased the solvent quality, resulting in phase separation of the reverse polyion–surfactant ion aggregates. By contrast, the L<sub>2</sub> phases in butanol, hexanol, and octanol could incorporate large fractions of water inside the reverse micelles.

Comparisons with previous studies showed that the geometry of the liquid crystalline phase in the ternary systems is mainly determined by the nature of the n-alcohol and to a lesser extent by the surfactant counterion. The restricted swelling by water for lamellar and hexagonal phases in systems with the polymeric counterions was interpreted as a consequence of the attractive forces between the aggregates due to bridging and ion correlation effects.

## ■ ASSOCIATED CONTENT

**S Supporting Information.** Compositions and SAXS-derived information (phase structure and structural parameters) for all of the systems investigated. This material is available free of charge via the Internet at <http://pubs.acs.org>.

## ■ AUTHOR INFORMATION

### Corresponding Author

\*E-mail: [wloh@iqm.unicamp.br](mailto:wloh@iqm.unicamp.br). Phone: + 55 19 3521 3148. Fax: + 55 19 3521 3023.

## ■ ACKNOWLEDGMENT

We thank the Brazilian Agencies FAPESP for financial support to this work and for a Ph.D. scholarship to J.S.B. and CNPq for support and for a senior researcher grant to W.L. The Brazilian Synchrotron Laboratory (LNLS) is also acknowledged for the use of the SAXS beamline and for the support of line staff. L.P. acknowledges support from the Swedish Research Council (VR) through the grant 239-2009-6794 to the Linnaeus Centre of Excellence on Organizing Molecular Matter (OMM).

## ■ REFERENCES

- (1) Svensson, A.; Piculell, L.; Cabane, B.; Ilekli, P. *J. Phys. Chem. B* **2002**, *106*, 1013.
- (2) Svensson, A.; Norrman, J.; Piculell, L. *J. Phys. Chem. B* **2006**, *110*, 10332.
- (3) Ilekli, P.; Piculell, L.; Tournilhac, F.; Cabane, B. *J. Phys. Chem. B* **1998**, *102*, 344.
- (4) Jönsson, B.; Lindman, B.; Holmberg, K.; Kronberg, B. *Surfactants and Polymers in Aqueous Solution*; John Wiley & Sons: West Sussex, England, 1998.
- (5) Laughlin, R. G. *The Aqueous Phase Behavior of Surfactants*; Academic Press: London, 1994.
- (6) Faul, C. F. J.; Antonietti, M. *Adv. Mater.* **2003**, *15*, 673.
- (7) Kabanov, A. V.; Bronich, T. K.; Kabanov, V. A.; Yu, K.; Eisenberg, A. *J. Am. Chem. Soc.* **1998**, *120*, 9941.
- (8) Svensson, A. V.; Johnson, E. S.; Nylander, T.; Piculell, L. *Appl. Mater. Interfaces* **2010**, *2*, 143.
- (9) Piculell, L.; Svensson, A.; Norrman, J.; Bernardes, J. S.; Karlsson, L.; Loh, W. *Pure Appl. Chem.* **2007**, *79*, 1419–1434.
- (10) Thalberg, K.; Lindman, B.; Karlstrom, G. *J. Phys. Chem.* **1991**, *95*, 6004.
- (11) Norrman, J.; Lynch, I.; Piculell, L. *J. Phys. Chem. B* **2007**, *111*, 8402.
- (12) Norrman, J.; Piculell, L. *J. Phys. Chem. B* **2007**, *111*, 13364.
- (13) Bernardes, J. S.; Loh, W. *J. Colloid Interface Sci.* **2008**, *318*, 411.
- (14) Bernardes, J. S.; Norrman, J.; Piculell, L.; Loh, W. *J. Phys. Chem. B* **2006**, *110*, 23433.
- (15) Fontell, K.; Khan, A.; Lindström, B.; Maciejewska, D.; Puang-Ngern, S. *Colloid Polym. Sci.* **1991**, *269*, 727.
- (16) Leal, C.; Bilalov, A.; Lindman, B. *J. Phys. Chem. B* **2006**, *110*, 17221.
- (17) Bernardes, J. S.; Da Silva, M. S.; Piculell, L.; Loh, W. *Soft Matter* **2010**, *6*, 144.
- (18) Hammersley, A. P.; Svensson, S. O.; Hanfland, M.; Fitch, A. N.; Häusermann, D. *High Pressure Res.* **1996**, *14*, 235.
- (19) Stephenson, R.; Stuart, J. *J. Chem. Eng. Data* **1986**, *31*, 56.
- (20) Stephenson, R.; Stuart, J.; Tabak, M. *J. Chem. Eng. Data* **1984**, *29*, 287.
- (21) Kunieda, H.; Shigeta, K.; Suzuki, M. *Langmuir* **1999**, *15*, 3118.
- (22) Kunieda, H.; Ozawa, K.; Huang, K.-L. *J. Phys. Chem. B* **1998**, *102*, 831.
- (23) Evans, D. F.; Wennerström, H. *The Colloidal Domain: Where Physics, Chemistry, Biology, and Technology Meet*, 2nd ed.; Wiley-VCH: New York, 1999.
- (24) Jönsson, B.; Wennerström, H. *J. Phys. Chem.* **1987**, *91*, 338.
- (25) Bernardes, J. S. *Equilíbrio de Fases e Caracterização Estrutural de Sistemas Contendo Poliânions e Surfatantes Catiônicos*. Ph.D. Thesis, University of Campinas, 2008.
- (26) Svensson, A.; Piculell, L.; Karlsson, L.; Cabane, B.; Jönsson, B. *J. Phys. Chem. B* **2003**, *107*, 8119.
- (27) Norrman, J.; Piculell, L. *J. Phys. Chem. B* **2007**, *111*, 13364.
- (28) Wei, X.; Fu, S.; Yin, B.; Sang, Q.; Sun, D.; Dou, J.; Wang, Z.; Chen, L. *Fluid Phase Equilib.* **2010**, *287*, 146.
- (29) dos Santos, S.; Gustavsson, C.; Gudmundsson, C.; Linse, P.; Piculell, L. *Langmuir* **2011**, *27*, 592.